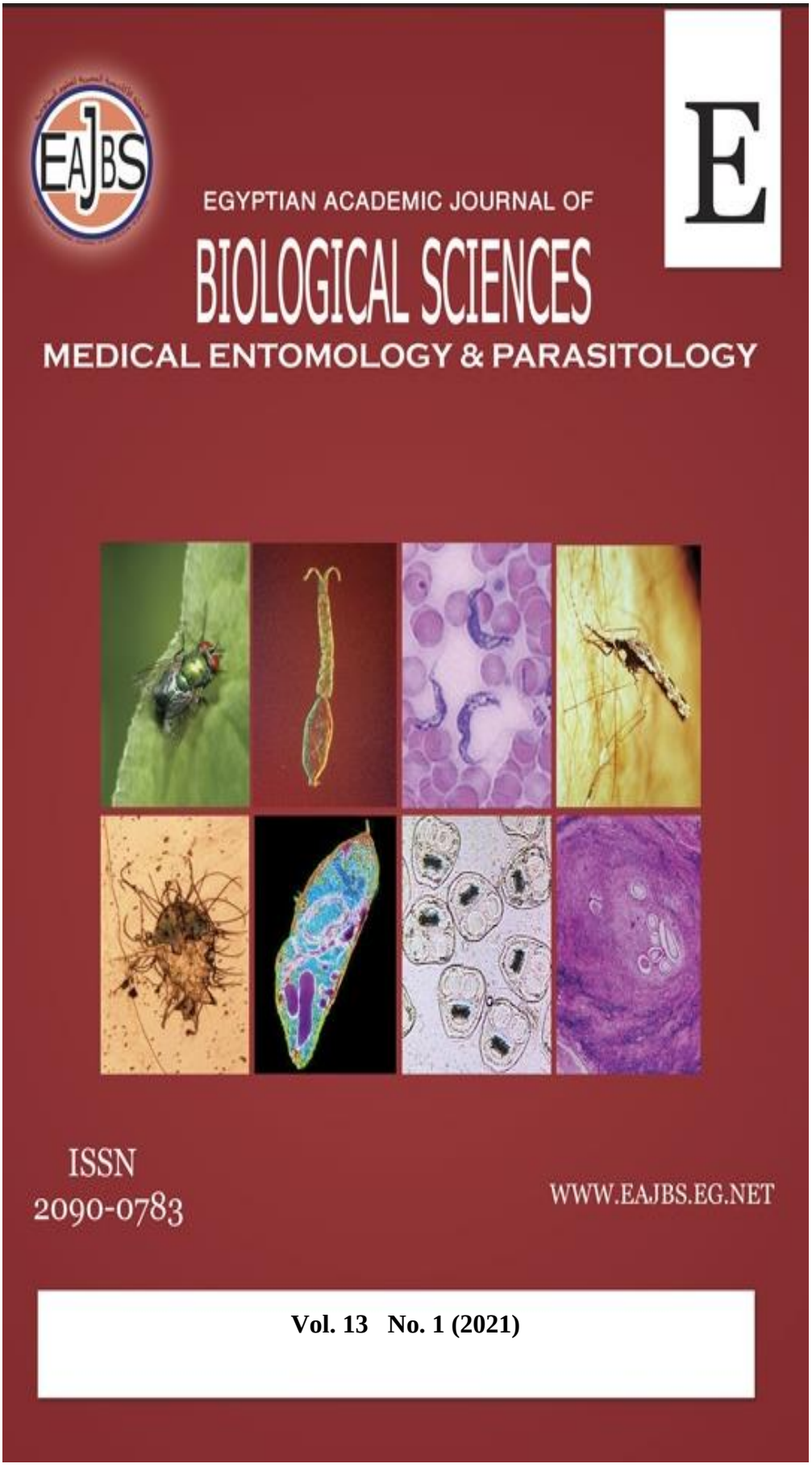

Citation: *Egypt. Acad. J. Biolog. Sci. (E-Medical Entom. & Parasitology Vol.13(1) pp 1-16(2021)*
DOI: 10.21608/EAJBSE.2021.134814

Egypt. Acad. J. Biolog. Sci., 13 (1):1 – 16 (2021)

Egyptian Academic Journal of Biological Sciences
E. Medical Entom. & Parasitology

ISSN: 2090 – 0783
www.eajbse.journals.ekb.eg

Two Coccidian Parasites and An Unusual Intraerythrocytic Cytoplasmic Vacuolar Inclusion from Agamid Lizard, *Trapelus savignii* in Egypt

Reda M. Mansour
Department of Zoology and Entomology, Faculty of Science, Helwan University, Egypt
E-mail : reda_mansour@science.helwan.edu.eg

ARTICLE INFO
Article History
Received:12/10/2020
Accepted:1/1/2021

Keywords:
Coccidia, Haemogregarines, *Sauroplasma*, *Isospora*, Agamidae.

ABSTRACT

Three types of parasites, two intraerythrocytic and one *Isospora* species, were recorded to infect lizard *Trapelus savignii* (Reptilia: Agamidae) collected in summer 2019 from the Eastern Desert in Egypt. The current intraerythrocytic parasites are haemogregarine species and unusual intraerythrocytic cytoplasmic vacuolar inclusions (ICVIs). Blood stages of haemogregarine species are differentiated into three forms; trophozoite, intermediate form, and mature gamont. Trophozoites measure 7.50–8.50 (8.10±0.30) × 2.20–2.40 (2.30±0.06) µm while intermediate forms and mature gamonts measure 7.89–10.39 (9.32±0.85) × 3.9–5.18 (4.32±0.45) and 8.87–12.13 (10.25±0.90) × 2.50–4.35 **(**3.45± 0.58**)** µm, respectively. ICVIs are un- or pale-stained with Giemsa and measure 1.62–5.45 (3.64±0.87) × 1.45–5.35 (3.51±1.10) µm. At the ultrastructure level, ICVIs appeared as a membrane-bound electron-lucent matrix and contain three types of materials according to their electron density that may resemble chromatin granules. No nucleus, Golgi apparatus, mitochondria, or any apical complex structure is observed within ICVIs. Effects of haemogregarine species and ICVIs on the infected erythrocytes are recorded. Exogenous and endogenous developmental stages of the present *Isospora* sp. are described. Sporulated oocysts are mostly spherical, contain bilayered wall, and measure 22.48–27.71 (25.47±1.81) × 21.69–26.91 (24.37±1.73). Oocyst residuum, polar granule and micropyle are absent. Sporocysts are ellipsoidal and measure 13.79–15.84 (14.97±0.67) × 8.80–11.03 (9.97±0.70). Stieda body is nipple-like while sub-Stieda body is absent. Multinucleate meronts contain up to 34 nuclei and measure 6.29–19.83 (11.91±4.58) × 5.43–10.76 (7.57±1.75). Developed microgamonts measure 16.59–18.89 (17.74±0.94) × 15.61–18.63 (17.12±1.24) while mature macrogamonts measure 16.34–24.27 (19.95±2.98) × 12.0–20.28 (16.92±3.22).

INTRODUCTION

Haemogregarines represent a group of heteroxenous intracellular blood parasites and are classified in suborder Adeleorina, order Eucoccidiorida, class Coccidia within the apicomplexan alveolates (Votýpka *et al.*, 2017). These protists include eight genera and their vertebral (intermediate) hosts are recorded from fishes to mammals (Davies and Johnston, 2000; Telford, 2009).

Dactylosoma and *Babesiosoma* infect fishes, toads and newts (Netherlands *et al.*, 2020) while *Cyrilia* and *Desseria* infect fishes, *Haemogregarina* infects fishes, turtles and possibly alligators, *Hemolivia* infects toads, lizards and tortoises, *Karyolosus* infects lizards, and *Hepatozoon* infects amphibians, reptiles, rare birds, and mammals (Smith, 1996; Davies and Johnston, 2000; Shazly, 2003; Telford, 2009). Haemogregarines infect primarily erythrocytes of their vertebrate hosts in addition to leukocytes in many cases of *Hepatozoon* spp. of mammals (Shazly, 2003). Five genera of haemogregarines, *Dactylosoma*, *Babesiosoma*, *Cyrilia*, *Haemogregarina*, and *Hemolivia*, undergo intraerythrocytic merogony and gamontogony while the remaining three genera, *Desseria*, *Karyolysus* and *Hepatozoon*, undergo only intraerythrocytic gamontogony (Davies and Johnston, 2000; Shazly, 2003; Telford, 2009).

Based on biological data and phylogenetic reconstruction, Karadjian *et al.* (2015) proposed a new classification for the terrestrial haemogregarines that extends to include *Hepatozoon* infecting mammalian carnivores, *Karyolysus* infecting reptiles, *Hemolivia* infecting reptiles and amphibians, in addition to the creation of a new genus, *Bartazoon*, infecting amphibians, reptiles, birds, and rodents. However, Maia *et al.* (2016) suggested that is still premature to finalize the systematic revision of haemogregarines as more molecular and biological data are needed. In Egypt, many haemogregarines were reported from lacertilian and ophidian hosts under the generic name *Haemogregarina* "sensu lato" (*s.l.*) and *Hepatozoon* (Bashtar *et al.*, 1984, 1987; Abdel-Ghaffar *et al.*, 1994; Al-Hoot and Abd-Al-Aal, 1999; Abdel-Haleem *et al.*, 2013).

The taxonomic status of intraerythrocytic cytoplasmic vacuolar inclusions (ICVIs) of lizards is a matter of controversy and their presence apparently shows low biodiversity among lacertilian reptiles. The majority of intraerythrocytic viral and bacterial inclusions are densely red-stained in Giemsa-stained blood films while so-called piroplasm inclusions are un- or pale-stained (Telford, 2009). Du Toit (1937) proposed a new piroplasmid genus, *Sauroplasma* to include small, rounded (typically ring-shaped) or irregularly shaped unpigmented intracytoplasmic parasites in erythrocytes of lizards. Telford (2009) defined reptilian piroplasmids as "chromatin granules associated with a vacuole or resemble a ring" and stated that *Sauroplasma* and *Serpentoplasma*, if they indeed piroplasms, show a little affinity to the mammalian piroplasms. Some authors assumed that the presence of so-called *Sauroplasma* spp. in lizards was overlooked or mistaken as artifacts or viral or bacterial infections and vice versa (Davies and Johnston, 2000; Telford, 2009; Ursula *et al.*, 2014).

Regarding the number of species, *Isospora* Schneider, 1881 is considered as the second largest biodiverse genus within the family Eimeriidae, after *Eimeria* Schneider, 1875 (Ghimire, 2010). *Isospora* species belong to order Eucoccidiorida, class Coccidia, phylum Apicomplexa, and most of their descriptions are based mainly on sporulated oocysts morphology (Berto *et al.*, 2011; Votýpka *et al.*, 2017). The sporulated oocysts of reptilian *Isospora* spp. are characterized by having two sporocysts with Stieda bodies and each sporocyst contains four sporozoites (Barta *et al.*, 2005). The majority of reptilian *Isospora* species is described from lizards than any other group and their endogenous stages are characterized by intranuclear or intracytoplasmic development mostly occurring within the small intestine of their hosts (Finkelman and Paperna, 2002). Mihalca *et al.* (2009) reviewed eleven *Isospora* species in agamid lizards. Five of them have intranuclear development and one species has intracytoplasmic development.

The agamid lizard *Trapelus savignii* Duméril and Bibron, 1837 is geographically

distributed in the Eastern Desert and Sinai of Egypt (Baha El Din, 2006). Many haemogregarines and isosporan infections were reported from different reptilian hosts in Egypt (Bashtar *et al.*, 1984, 1987; Shazly, 2000; Mansour and Abou Shafeey, 2019) but not from agamid lizard *Trapelus savignii* yet. However, a suggested new *Caryospora* sp. is reported from lizard *Trapelus savignii*, recently (Mansour, 2020). The current study aims to investigate and discuss the characteristic features of intraerythrocytic blood parasites and developmental stages of *Isospora* species from Savigny's Agama *Trapelus savignii* in Egypt.

MATERIALS AND METHODS

Experimental Animals:

One hundred and three agamid lizards *Trapelus savignii* Duméril and Bibron, 1837 (Agamidae: Sauria: Reptilia) were collected in summer 2019 from the Egyptian Eastern Desert and transported to the laboratory of Parasitology and invertebrates at Zoology and Entomology Department, Faculty of Science, Helwan University, where they were investigated for the presence of blood parasites and coccidian infections.

Light microscopic studies:

Morphological characterizations of the current intraerythrocytic parasites and *Isospora* species were examined and photographed under an oil immersion lens (1000X) using a Zeiss research photomicroscope. Measurements are expressed in micrometers (µm) and presented by the range of length × width and then followed by the mean values ± standard deviation in parentheses.

1- Examination of blood parasites:

Thick and thin blood films were prepared from lizard tails. Blood smears were air-dried, fixed in absolute methanol (5 min), stained with 3% phosphate-buffered Giemsa stain (pH 7.3) for 30 minutes, dehydrated in ascending series of ethanol, cleared in xylene, and mounted in Canada balsam.

2- Examination of isosporan infection:

a- Investigation of oocysts (exogenous stages):

The abdomen of each lizard was gently squeezed to get fecal particles. Obtained faeces were carried by forceps on a clean slide. The investigation of the present isosporan oocysts was carried out by direct fecal smears or by mixing and diluting of faeces in a drop of distilled water. The oocysts in intestinal contents of *Isospora*-positive lizards are concentrated by flotation technique following Long *et al.* (1976).

b- Investigation of merogonic and gamogonic stages (endogenous stages):

Pieces measuring about 5 mm were taken from the stomach, small intestine, liver, kidney, spleen and rectum of the *Isospora*-infected lizards and were immediately fixed in 10% phosphate-buffered formalin (pH 7.3) for at least 12 hours at 4^0 C. After 3-4 washings in the phosphate buffer for 10-15 min each, the specimens were dehydrated in ethanol ascending series, cleared in xylene, embedded in parablast and sectioned by a rotatory microtome at thickness of 5 µm. Then, sections were deparaffinized, hydrated in ethanol descending series, stained with haematoxylin and eosin stain, dehydrated in ascending ethanol series and cleared in xylene again, and finally covered by a coverslip with Canada balsam.

Transmission electron microscopy (TEM) of ICVIs:

Blood samples of the infected lizards were primary fixed in 3% (v/v) glutaraldehyde buffered in 0.1M sodium cacodylate buffer (pH 7.3) for at least 4 hours. Then, fixed specimens were washed in buffer three times (15 min for each) and secondary fixed with 1% osmium tetroxide buffered in 0.1M sodium cacodylate buffer for 2 hours. Afterward, specimens were dehydrated in ascending ethanol series, embedded in epoxy resin, sectioned into semithin sections (1 µm thick), and stained with toluidine blue stain. Ultra-thin sections (50-80 nm thick) were cut using a Leica Ultracut UCT Ultramicrotome, stained with uranyl acetate for 20 min and alkaline lead citrate 2-3 min (Reynolds 1963) and finally examined by a JEOL-JEM 1010 TEM at the

Regional Center for Mycology and Biotechnology, Al-Azhar University, Cairo, Egypt.

RESULTS

I- Intraerythrocytic parasites (Figs. 1 and 2):

A- Haemogregarine species (Figs. 1a-f):

(1)- Prevalence and level of parasitaemia:

Out of one hundred and three examined lizards *Trapelus savignii*, only one male (0.97 %) was found to be naturally infected with haemogregarine sp. on the initial examination. The level of parasitaemia (numbers of haemogregarine-infected erythrocytes/1000 erythrocytes) was generally low and recorded as 1.80 %.

(2)- Blood stages of the parasite:

The blood stages of the present haemogregarine are differentiated into three forms; the small, intermediate, and mature forms. The nucleus of parasite is usually obvious and the cytoplasm is free of granules or vacuoles. The small form or trophozoite (n = 12) is the thinnest stage and has a nucleus located near its pointed end while the opposite end is broad (Fig. 1a). It measures 7.50–8.50 (8.10±0.30) × 2.20–2.40 (2.30±0.06) with a shape index or length/width (L/W) ratio of 3.38–3.62 (3.52±0.08). The intermediate form (n = 22) appears usually thicker, slightly curved, and dwarf (Figs. 1b-d). It measures 7.89–10.39 (9.32±0.85) × 3.90–5.18 (4.32±0.45) with a relatively smaller L/W ratio of 1.52–2.66 (2.19±0.39). The mature form or mature gamont (n = 28) is typically banana-shaped (Figs. 1f and g) showing a considerable degree of curvature. It measures 8.87–12.13 (10.25±0.90) × 2.50–4.35 **(**3.45± 0.58**)** with L/W ratio of 2.50–4.38 **(**3.15±0.55). The nucleus of mature gamont is stained dark violet with Giemsa and measures 2.06–3.19 (2.75±0.38) × 2.60–3.56 (3.11±0.30) with L/W ratio of 0.80–1.05 (0.88±0.08). The parasites lay parallel (Figs. 1a, e, and f) or take apical positions in regard to erythrocytes nuclei (Figs. 1b and d). Parasitophorous vacuoles are scarcely noticed in most cases between the parasite and host cell cytoplasm.

(3)- Effects of haemogregarine on infected erythrocytes:

Blood forms of the current haemogregarine are erythrocytic invaders. No extracellular stages are noticed and leucocytes aren't infected. The infected erythrocytes contain only one parasite. Uninfected erythrocytes (n = 60) have an elliptical shape, measure 13.53–18.44 (15.79±1.15) × 6.67–9.14 (7.97±0.49) with L/W ratio of 1.53–2.49 (1.99±0.21) and contain a centrally located nucleus measuring 5.21–7.14 (6.37± 0.50) × 2.96–4.43 (3.70±0.35) with L/W ratio of 1.30–2.34 (1.74±0.25). Generally, the infected erythrocytes (n = 60) show slight hypertrophy (Figs. 1b and f), no dehaemoglobinization, and measure 11.77–18.36 (16.14±1.95) × 7.39–11.85 (9.14±1.14) with L/W ratio of 1.01–2.48 (1.81±0.37). Infected erythrocytes also show shape distortion (Fig. 1c) and a constriction between an erythrocytic region containing parasite and another region containing erythrocytic nucleus (Fig. 1d). In rare cases, the infected erythrocyte is smaller than uninfected ones (Fig. 1e). The nuclei of infected erythrocytes are not fragmented, mostly elongated, displaced laterally or terminally and decreased slightly in width measuring 6.09–8.89 (7.84 ±0.74) × 2.30–3.76 (3.07±0.38) with L/W ratio of 1.78–3.79 (2.61±0.49).

B- Intraerythrocytic cytoplasmic vacuolar inclusions (ICVIs):

(1)- Prevalence and level of parasitaemia:

Five lizards (5/103, 4.85 %) were found to contain ICVIs in their peripheral blood. Prevalence was higher in males (3/58, 5.17 %) than females (2/45, 4.44 %). The level of parasitaemia (numbers of ICVIs-contained erythrocytes/1000 erythrocytes) was generally high and recorded from 25 % to 90 %.

(2)- Light microscopy of ICVIs (Figs. 1d, g, and h):

ICVIs are seen inside the cytoplasm of erythrocytes and probably proerythrocytes. No extracellular or leukocytic stages are noticed. Normally, the

infected blood cell contains only one ICVI (Figs. 1d, g and h), but occasionally, up to four ICVIs are seen within the cytoplasm of a single erythrocyte (Fig. 1h). Under light microscopy, these ICVIs are un- or pale-stained with Giemsa and vary in shape from crescent rod-shape to triangular, quadrate, spherical, subspherical, oval and irregular shape. ICVIs (n = 100) measure 1.62–5.45 (3.64±0.87) × 1.45–5.35 (3.51±1.10) and in some cases, they are seen in erythrocytes infected by the present haemogregarine (Fig. 1d).

(3)- Transmission electron microscopy (TEM) of ICVIs (Fig. 2):

At ultrastructural levels, ICVIs acquired many different shapes. They are nearly ovoid with a shape index of 1.12-1.23 (Figs. 2a-c, g and i), ellipsoid with shape index of 1.41-1.58 (Figs. 2d-f), slipper-like (Figs. 2h and j), kidney-shaped (Fig. 2k) or resemble bean seed embryo (Fig. 2l). Some ICVIs are seen neighboring eleven relatively small vacuoles (Fig. 2a). However, many ICVIs are noticed to have envelopes thickened by moderate electron-dense materials (Figs. 2b, c, e, f, i, k, and l). Within the electron-lucent matrix of these ICVIs, three types of materials are noticed according to their electron density. They are highly, moderately, or low electron-dense materials that may resemble chromatin granules. The highly electron-dense materials are found in form of relatively fine dispersed particles (Figs. 2a, c, g, h, k and l), rounded globules (Fig. 2e), or short beaded-like string (Fig. 2c). The highly electron-dense materials are mostly seen associated with moderately electron-dense materials (Figs. 2a, c, e, f and l). The envelope of one ICVI is seemed to invaginate and internalize some of the exposed substances in behavior that resembles endocytosis (Fig. 2b). However, another ICVI is seemed to be in endo- or exo-cytic process (Fig. 2i). Low electron-dense materials are seen in some ICVIs (Figs. 2d and e). In addition, some ICVIs are observed in a process resembling budding or fission (Fig. 2g) while others have process-like structures (Figs. 2k and i).

(4)- Effects of ICVIs on infected erythrocytes:

Under light microscopy, most of the ICVIs-contained erythrocytes are of normal size and shape but some are slightly wider than normal (Figs. 1g and h) measuring 13.35–18.7 (16.34±1.37) × 8.4–10.36 (9.53 ± 0.49) with L/W ratio of 1.41–2.04 (1.72±0.16). The nuclei of ICVIs-contained erythrocytes are usually smaller than normal measuring 4.07–7.12 (5.32±0.73) × 2.86–3.86 (3.30±0.28) with L/W ratio of 1.07–2.2 (1.62±0.27). At the ultrastructural level, membranes of infected erythrocytes become concaved around these ICVIs (Figs. 2f-i).

II- Intestinal coccidian parasite:

A- *Isospora* species (Fig. 3):

1- Prevalence:

The overall prevalence for the present *Isospora* sp. is 13.59 % (14/103). The infection rate is higher in females (8/45, 17.78 %) than males (6/58, 10.34 %).

2- Exogenous stages or oocysts (Figs. 3a-e):

Unsporulated oocysts are not observed. However, oocysts are noticed with sporoblasts (Figs. 3a and b), during sporozoites formation (Fig. 3c), or with fully formed sporocysts (Figs. 3d and e) in host faeces. Sporoblasts measure 10.29–12.41 (11.12±0.80) × 9.25–10.25 (9.68±0.38) and usually fill less than one-half of oocysts cavity. On one occasion, abnormal sporulation is recorded and a third elliptical sporoblasmic material is noticed measuring 9.06 × 6.02 (Fig. 3b). The sporulated oocysts (n = 50) are usually spherical (85 %) and rarely subspherical (15 %) measuring 22.48–27.71 (25.47±1.81) × 21.69–26.91 (24.37±1.73) with a shape index of 1.01–1.13 (1.05±0.04). Occasionally, one oocyst is noticed to have an ovoid shape measuring 28.60–23.02 with a shape index of 1.24 and this oocyst is supposed to occur under mechanical pressure during specimen preparation (Fig. 3e). The oocyst wall is smooth, bi-layered and measures 1.42–1.78 (1.59±0.12). The outer layer of oocyst wall is relatively thick, not pitted or striated, somewhat colorless or faintly green and

measure 0.76–1.06 (0.90±0.13) while the inner layer is relatively thin, darkly grey and measure 0.52–0.78 (0.68±0.08). Oocyst residuum, polar granule and micropyle are not observed.

The fully developed sporocysts (Figs. 3d and e) are ellipsoidal in shape, fill most of the concavity of oocyst and measure 13.79–15.84 (14.97±0.67) × 8.80–11.03 (9.97±0.70) with a shape index of 1.38–1.61 (1.5±0.08). Stieda body is obvious, knob- or nipple-like and measures 0.70–1.22 (0.93±0.17) high × 1.43–2.15 (1.80±0.26) wide. Sub-Stieda body is absent. Sporocyst wall is smooth, single-layered and measures 0.40–0.48 (0.43±0.03). Sporocyst residuum is a compact mass of 12–32 finely granules lying centrally or peripherally to sporozoites and measures 7.03–9.10 (8.03±0.70) × 5.61–7.95 (6.83±0.79). The sporozoites are elongate banana-shaped measuring 9.15–12.65 (10.90±1.43) × 2.20–2.81 (2.51±0.25) with a shape index of 4.15–4.51 (4.34±0.15). Sporozoite has a relatively large central nucleus measuring 2.56–3.27 (2.91±0.29) × 2.51–2.72 (2.61±0.9) and two smaller peripherally-located refractile bodies, each measure 1.62–1.75 (1.69±0.05) × 1.35–1.50 (1.43±0.06).

3- Site of infection and endogenous stages (Figs. 3f-q):

Most of the endogenous (merogonic and gamogonic) stages of the present *Isospora* sp. occurred in enterocytes of the small intestine of their host taking apical positions in regard to enterocytes nucleus. Few stages were recorded in *lamina propria* of the small intestine. The majority of these stages are seen within clear parasitophorous vacuoles. Uninucleate meronts are usually ovoidal (Fig. 3f), contain a central nucleus and measure 4.40–6.36 (5.38±0.80) × 3.61–4.77 (4.19±0.47) with a shape index of 1.22–1.33 (1.28±0.05). Binucleate meronts are spheroidal (Fig. 3g) and measure 4.88–8.33 (6.60±1.41) × 4.82–7.95 (6.38±1.28) with shape index of 1.01–1.05 (1.03±0.01) while quadrinucleate meronts are spherical to ovoid (Fig. 3h) and measure 8.89–9.44 (9.24±0.25) × 7.64–9.22 (8.34±0.66) with shape index 1.02–1.23 (1.11±0.09). Occasionally, two quadrinucleate meronts are seen within the same infected enterocyte (Fig. 3h). Multinucleate meronts, with more than 4 nuclei, extend from subspherical to elongate ellipsoidal (Figs. 3i-k). They contain up to 34 nuclei and measure 6.29–19.83 (11.91±4.58) × 5.43–10.76 (7.57±1.75) with a shape index of 1.08–1.96 (1.53±0.30). Merozoites are seen randomly-distributed (Fig. 3l) or arranged in a rosette form around a residual body (Fig. 3m). The observed merozoites are slender and crescent-shaped measuring 3.65–6.28 (5.27±0.81) × 1.00–1.62 (1.39±0.27) with a shape index of 3.25–6.27 (3.92±1.06).

Developed microgamonts are noticed and characterized by the presence of many randomly distributed small nuclei (Figs. 3n and o). Microgamonts with 12–16 nuclei (Fig. 3n) are spherical to ovoid measuring 10.61–14.07 (12.40±1.42) × 9.55–13.66 (11.27±1.74) with shape index of 1.03–1.18 (1.11± 0.06) while those with 40–48 nuclei (Fig. 3o) are spherical measuring 16.59–18.89 (17.74±0.94) × 15.61–18.63 (17.12±1.24) with shape index of 1.01–1.06 (1.04±0.02). Developed and mature macrogamonts are also described (Figs. 3p and q). Developed macrogamont is characterized by the beginning of the appearance of wall forming bodies (Fig. 3p). It has a subspherical shape, relatively small size, central nucleus, and measures 6.02–9.55 (7.79±1.44) × 5.51–8.97 (7.24±1.41) with a shape index of 1.06–1.09 (10.8±0.01). Mature macrogamont is characterized by having a larger number of wall bodies that may reach up to 60 (Fig. 3q). It has a subspherical to somewhat elliptical shape, larger size, bigger central nucleus and measures 16.34–24.27 (19.95±2.98) × 12.0–20.28 (16.92±3.22) with a shape index of 1.084–1.35 (1.19±0.09).

````
````

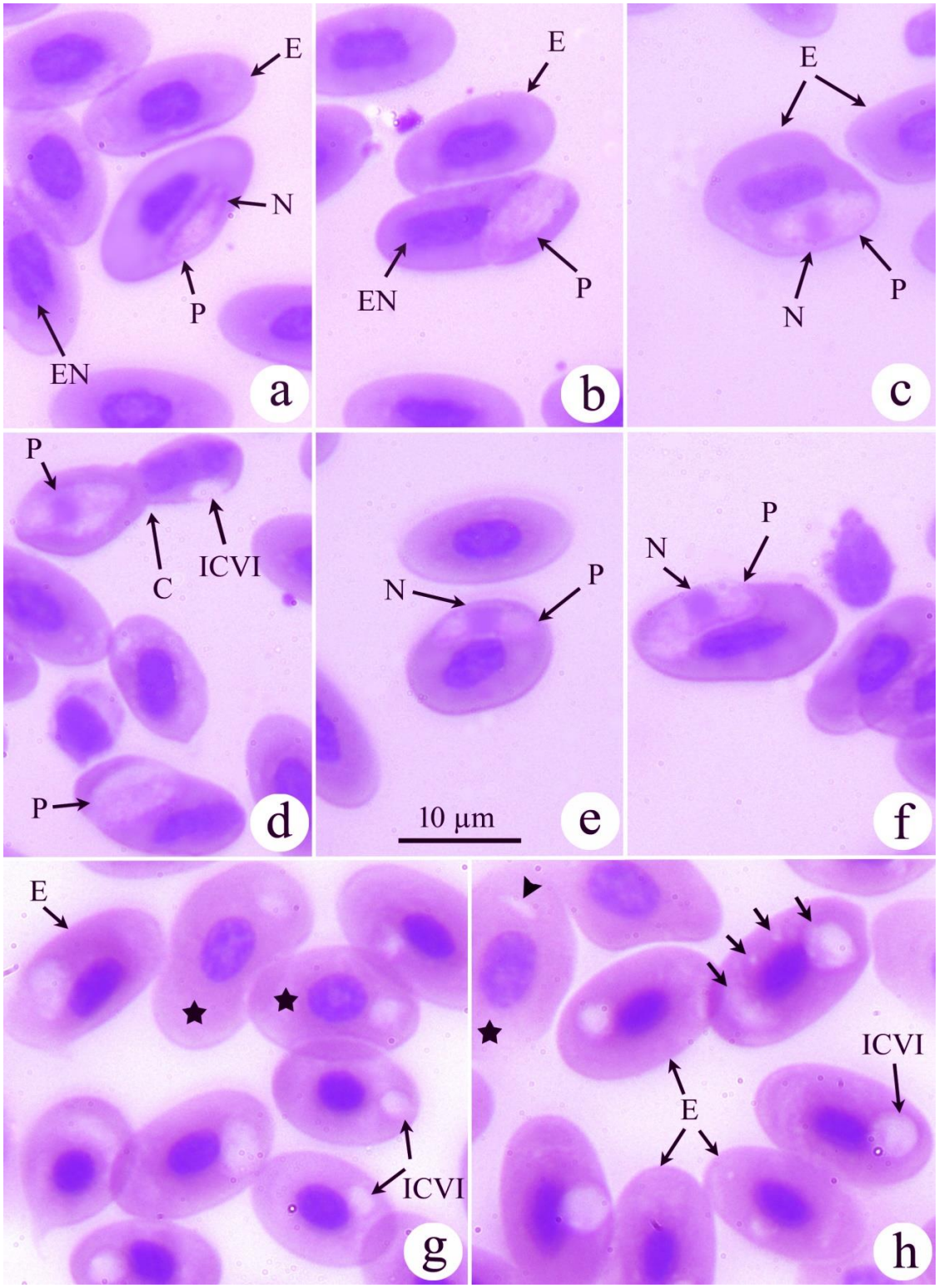

Fig. 1: Photomicrographs of erythrocytes containing present haemogregarine **(a-f)** and ICVIs **(g, h)**. **(a-f)** Erythrocytes infected by small **(a)**, intermediate forms **(b-d)** and mature gamonts **(e, f)**. Note the elongation **(b)**, shape distortion **(c)**, constriction **(d)**, small size **(e)** and hypertrophying **(f)** of the infected erythrocytes. **(g, h)** Erythrocytes and probably proerythrocytes (asterisks) contain mostly rounded to ellipsoid ICVIs. Note presence of a rod-shaped ICVI (arrow head) and four different-sized ICVIs (short arrows) in the infected blood cells **(h)**. **Abbreviations:** C, constriction; E, erythrocytes; EN, erythrocyte nucleus; ICVI, intraerythrocytic cytoplasmic vacuolar inclusion; N, parasite nucleus; P, parasite. Scale bar = 10 µm.

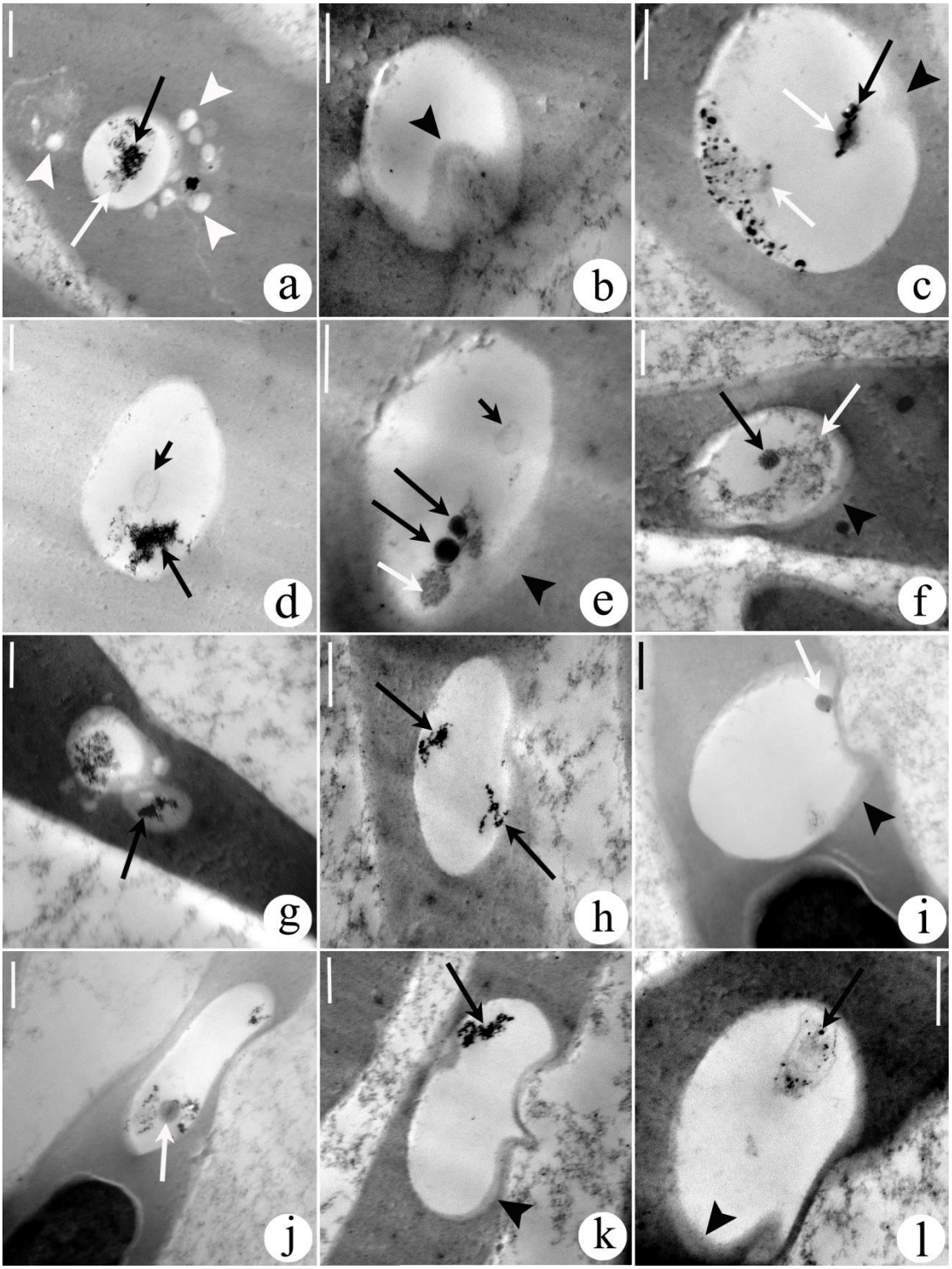

Fig. 2: Transmission electron micrographs of ICVIs. **(a-c, g, i)** Nearly oval ICVIs. Note presence of 11 tiny vacuoles (white arrow heads) neighboring to the ICVI **(a)** and ICVI envelope is seemed to internalize substances like as in endocytosis **(b)**. **(d-f)** Elliptical ICVIs. **(g)** The ICVI appeared to be in budding or fission process. **(h, j)** Slipper-like ICVIs. **(i)** The ICVI seemed to be in endo- or exo-cytic process. **(k)** Kidney-shaped ICVI with a lateral process. **(l)** ICVI resemble bean seed embryo. Note that the erythrocytes membranes become concaved around ICVIs **(g-l)**. Within ICVIs matrix, highly (long black arrows), moderately (white arrows) and/or low (short black arrows) electron-dense materials are present. Most ICVIs have thickened envelope (black arrow head). Scale bar = 0.5 μm.

````
````

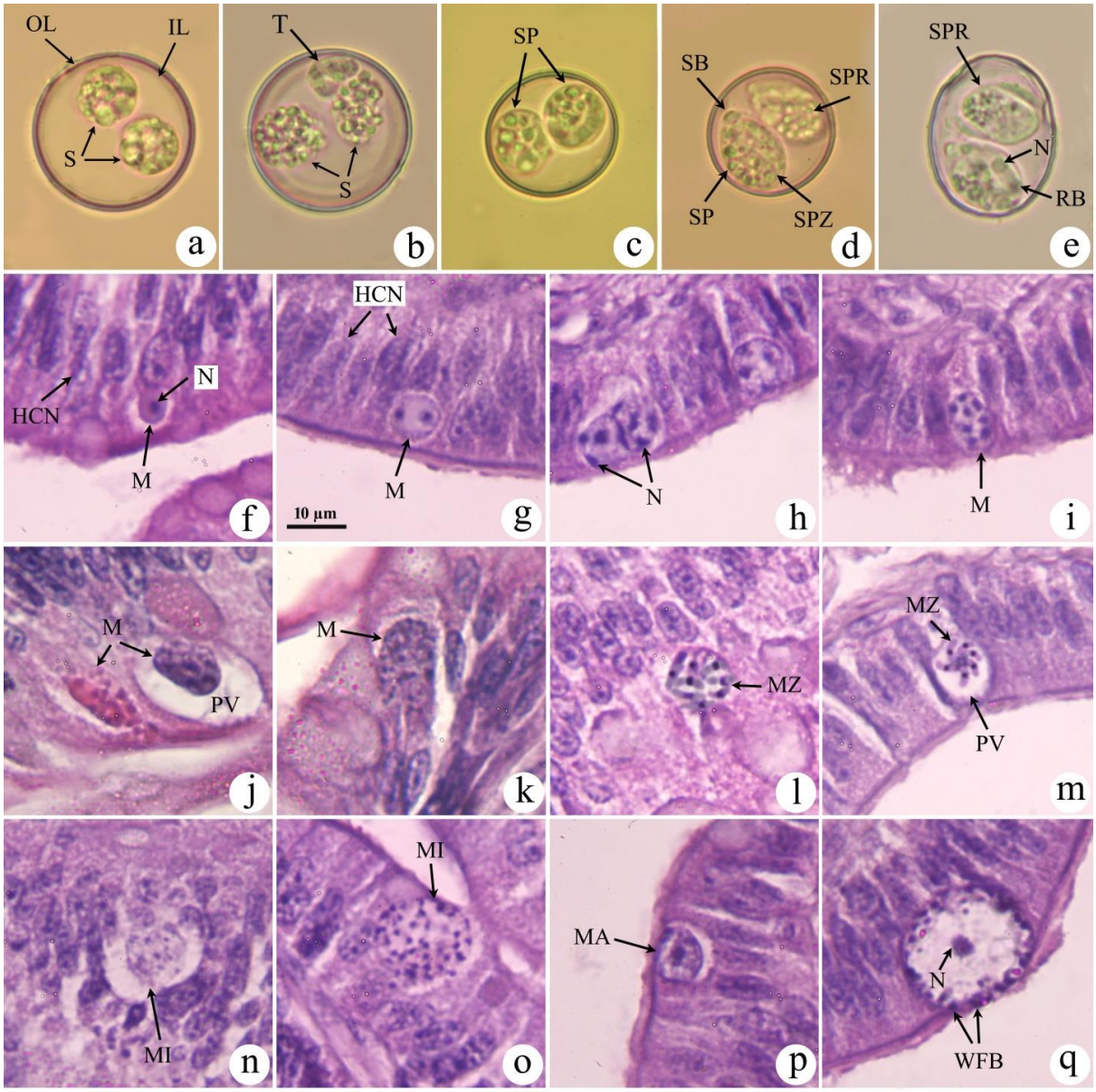

Fig. 3: Photomicrographs of the developmental stages of the present *Isospora* sp. **(a-e)** Exogenous stages. **(f-q)** Endogenous stages infecting small intestine of host. **(a)** Double-walled oocyst with 2 sporoblasts. **(b)** Oocyst with abnormal sporulation showing 2 sporoblasts and a third sporoblasmic structure. **(c)** Oocyst with 2 sporocysts during sporozoites formation. **(d, e)** Sporulated oocysts showing 2 sporocysts, Stieda body, sporocyst residuum and sporozoites. Note presence of single nucleus and 2 refractile bodies in sporozoite **(e)**. **(f-h)** Intestinal tissues infected with uninucleate **(f)**, binucleate **(g)** and multinucleate **(h-k)** meronts with different number of nuclei. **(l, m)** Intestinal cells contained mature meront with eight **(l)** and six merozoites **(m)**. **(n, o)** Intestinal cells contained developed microgamonts with different number of nuclei. **(p, q)** Intestinal cells contained developed **(p)** and mature **(q)** macrogamonts. **Abbreviations:** HCN, host cell nucleus; IL, inner oocyst wall; M, meront; MA, macrogamont; MI, microgamont; MZ, merozoites; N, nucleus of parasites; OL, outer oocyst wall; PV, parasitophorous vacuole; RB, refractile body; S, sporoblast; SB, Stieda body; SP, sporocyst; SPR, sporocyst residuum; SPZ, sporozoites; T, third sporoblasmic structure; WFB, wall forming bodies. Scale bar = 10 µm.

Table 1: Comparative measurements (in μm) of haemogregarines blood stages of some lizards.

- Parasite (reference)	- Type host (type locality)	- Prevalence - Parasitaemia	- Intraerythrocytic blood forms	- Effects on IE, IEN
***Haemogregarina damiettae* (Abdel-Haleem *et al.*, 2013)**	- *Acanthodactylus boskianus* (Damietta, Cairo G., Egypt)	- 30 / 50(60 %) - No data	- YF: 9–12 (10) × 2–5 (3) - MG: 16–22 (18) × 4–7 (5)	- EH, ED - IENE, IENL/T, IENF
***Haemogregarina* sp. (Abdel-Ghaffar *et al.*, 1994)**	- *Ptyodactylus hasselquistii* (Giza G., Egypt)	- 30 / 70(42.9 %) - No data	- YF: 10.0±0.3 × 5.1±0.6 - MG: 24.3±0.6 × 8.5±1.2	- EH - IENL/T
***Haemogregarina* sp. (Al-Hoot and Abd-Al-Aal, 1999)**	- *Varanus niloticus* (Toshka, Upper Egypt)	- 3 / 7(42.8 %) - No data	- YF: 6.75±0.04 × 3.02±0.07 - IF: 9.07±0.03 × 3.72±0.06 - MG: 12.05±0.2 × 2.7±0.14	- EH, ED - IENE, IENL/T
Haemogregarine sp. (Abou Shafeey *et al.*, 2019)	- *Scincus scincus* (South Sinai desert, Egypt)	- 8 / 20 (40 %) - Up to 25–40 %	- YF: 13.2±0.4 × 3.5±0.15 - MG: 16.3±1.4 × 5.2±0.4	- EH - IENL/T
***H. affluomaloti* (Van As *et al.*, 2015)**	- *Pseudocordylus melanotus* (Eastern Free State, South Africa)	- 24 / 69(34.8 %) - Up to 17 %	- IG: 11.0 × 3.5 - MG: 15.8–21.8 (18.7±1.4) × 3.2–7.3 (5.7±0.9)	- EH, ED (in one host) - IENE, IENL/T, IENF
***H. gracilis* (Bashtar *et al.*, 1987)**	- *Trachylepis quinquetaeniata* (Giza G., Egypt)	- 168 / 420(40 %) - Up to 40–50 %	- YF: 12.75±1.4 × 0.85±0.05 - MG: 21.3±1.52 × 1.14±0.2	- EH, ED - IENL/T
***H. kisrae* (Paperna *et al.*, 2002)**	- *Stellagama stellio* (Olive grove at Kisra, southeast Samaria, Palestine)	- 9 / 27(33.3 %) - Up to 9 %	- YF: 6–8 × 4–5 (oblong type); 7–9 × 5–6 (oval type) - IF: 7–11 × 5–7 - MG: 12–15 × 2–5.5	- EH - IENL/T
***H. langii* (Van As *et al.*, 2013)**	- *Pseudocordylus langi* (Eastern Free State, South Africa)	- 13 / 13(100 %) - Up to 1.8 %	- IG: 10.7–14.4 (12.7±1.4) × 3.2–4.6 (3.8±0.5) - MG: 15.4–28.1 (19.1±1.0) × 3.5–7.9 (6.2±1.1)	- EH, ED - IENE, IENL/T
***H. stellio* (Shazly, 2000)**	- *Stellagama stellio* (Alexandria G., Burg Al-Arab, Abu-Rawash, Egypt)	- 23 / 40(57.5 %) - Up to 85 %	- YF: 13.2±0.7 × 4.1±0.2 - MF: 17.5±1.2 × 5.6±0.7	- EH - IENL/T
***H. vacuolatus* (Van As *et al.*, 2013)**	- *Pseudocordylus langi* (Eastern Free State, South Africa)	- 3 / 13(23.1 %) - Up to 2 %	- IG: ~ 11.1 × 3.8 - MG: 14.7–17.6 (16.5±1.0) × 4.0–7.7 (5.9±1.2)	- EH, ED - IENE, IENL/T
Haemogregarine sp. (present species)	- *Trapelus savignii* (Eastern Desert, Egypt)	- 1 / 103 (.97 %) - 1.8 %	- YF: 7.5–8.5 (8.1±0.3) × 2.2–2.4 (2.3±0.06) - IF: 7.89–10.39 (9.32±0.85) × 3.9–5.18 (4.32±0.45) - MG: 8.87–12.13 (10.25±0.9) × 2.5–4.35 (3.45±0.58)	- EH - IENL/T

Abbreviations: ED, erythrocytes dehaemoglobinization; EH, erythrocyte hypertrophy; G., Governorate, *H.*: *Hepatozoon*; IE, infected erythrocytes; IEN, infected erythrocyte nucleus; IENE, infected erythrocyte nucleus enlargement; IENF, infected erythrocyte nucleus fragmentation; IENL/T, infected erythrocyte nucleus displaced laterally or terminally; IF, intermediate form; IG, immature gamont; MG, mature gamont; YF: youngest form (trophozoite).

DISCUSSION

Many haemogregarines are recorded from lacertilian hosts in Egypt (Bashtar *et al.*, 1987; Abdel-Ghaffar *et al.*, 1994; Al-Hoot and Abd-Al-Aal, 1999; Abdel-Haleem *et al.*, 2013) and the present species is recorded for the first time from the agamid lizard *Trapelus savignii* in Egypt. It represents one of the terrestrial haemogregarines but in absence of molecular data, it is hard to locate it under a specific generic name. The prevalence of present haemogregarine sp. is low for a reptilian host recording 0.97 %. The present parasite is compared with other haemogregarines reported from some saurian hosts in prevalence, parasitaemia level, measurements of intraerythrocytic forms, and effects on infected erythrocytes (Table 1). Three erythrocytic blood forms are

recorded for the current parasite. Similar observations are noticed in *Haemogregarina* and *Hepatozoon* species (Al-Hoot and Abd-Al-Aal, 1999; Paperna *et al.*, 2002). However, only two blood forms are also reported (Bashtar *et al.*, 1987; Abdel-Ghaffar *et al.*, 1994; Shazly, 2000) (see Table 1).

Like the majority of terrestrial haemogregarines (Table 1), mature gamonts of the present species are typically banana-shaped with non-pigmented cytoplasmic granules. In addition, single erythrocytic infection is only recorded and intraerythrocytic merogony is absent. Similar observations were reported in many reptiles infected by *Haemogregarina* and *Hepatozoon* species (Al-Hoot and Abd-Al-Aal, 1999; Shazly, 2000; Abdel-Haleem *et al.*, 2013; Van As *et al.*, 2013). However, leucocytes were recorded as the main site of gamont infection for mammalian haemogregarines (Smith, 1996). In addition, Hussein (2006) recorded single and double haemogregarine infections in both erythrocytes and leucocytes of the infected gecko *Ptyodactylus hasselquistii* from Qena in Egypt. Double infection was also noticed for some haemogregarine infections (Bashtar *et al.*, 1987; Al-Hoot and Abd-Al-Aal, 1999; Abdel-Haleem *et al.*, 2013; Abou Shafeey *et al.*, 2019).

The present species causes slight erythrocyte hypertrophy and erythrocytic nucleus elongation that displaced laterally or terminally. Moreover, Cytoplasm dehaemoglobinization and nucleus fragmentation are not observed. Similar observations were noticed in many saurian hosts infected by haemogregarines (Abdel-Ghaffar *et al.*, 1994; Shazly, 2000; Abou Shafeey *et al.*, 2019) (Table 1). However, dehaemoglobinization and nucleus fragmentation were observed in erythrocytes of some lacertilian hosts such as *Acanthodactylus boskianus* infected by *Haemogregarina damiettae* (Abdel-Haleem *et al.*, 2013) and *Pseudocordylus melanotus* infected by *Hepatozoon affluomaloti* (Van As *et al.*, 2015).

ICVIs of the present lizard are rarely- or un-stained. Some authors follow the suggestion of Du Toit (1937) and attribute pale- or un-stained ICVIs of lizards to genus *Sauroplasma* (Svahn, 1976; Alberts *et al.*, 1998; Telford, 2009; Ursula *et al.*, 2104). Ultrastructure findings of the present ICVIs showed the absence of nucleus, mitochondria, Golgi apparatus and other structures distinctive for eukaryotic cell and this may support the hypothesis proposed by Davies and Johnston (2000) that genus *Sauroplasma* is not of protistan origin. However, all examined transmission electron micrographs of the current study showed no packed viral or bacterial particles within these ICVIs. In addition, the presence of a process resembling endo- or exo-cytosis for the present ICVIs is considered a matter of controversy as this behavior is characteristic for eukaryotic cells and scarcely found in bacteria (Fuerst and Sagulenko, 2010; Mills, 2020). Moreover, three types of materials according to their electron density that may resemble chromatin granules were seen dispersed in the electron-lucent matrix of the present ICVIs. Furthermore, electron micrographs do not reveal any apicomplexan structures. Similar observations were noticed in transmission electron micrographs for other so-called *Sauroplasma* spp. (Alberts *et al.*, 1998; Van As, 2012).

Mansour and Abou Shafeey (2019) compiled seven named *Isospora* species from the saurian hosts in Egypt. These include three species from *Chalchides ocellatus*, two species from *Acanthodactylus* spp., one species from *Trachylepis vittati* and one species from *Stenodactylus elegans*. The prevalence of the current *Isospora* sp. is relatively low recording 13.59 %. Similar observations of low rates of natural infection were reported for *I. cannoni* (12.50 %), *I. choochotei* (11.54 %) (Finkelman and Paperna, 1994), *I. farahi* (12.50 %) (Mihalca *et al.*, 2009) and *I. vittati* (24.07 %) (Mansour and Abou Shafeey, 2019). However, higher rates were recorded for *I. chalchidis* (74.19 %), *I. eimanae* (54.84 %) (Amoudi, 1989), *I. ameivae* (70.59 %) and *I.*

hemidactyli (63.64 %) (Lainson and Paperna, 1999).

Sporulated oocysts of current *Isospora* sp. are spherical to subspherical. Similar records were noticed for *I. choochotei* (Finkelman and Paperna, 1994), *I. farahi* (Mihalca *et al.*, 2009) and *I. vittati* (Mansour and Abou Shafeey, 2019). However, oocysts of *I. chalchidis*, *I. eimanae* (Amoudi, 1989) and *I. deserti* (Finkelman and Paperna, 1994) are only spherical. In addition, oocysts of *I. cannoni* (Finkelman and Paperna, 1994) and *I. ameivae* (Lainson and Paperna, 1999) have only subspherical shapes. Moreover, oocysts of *I. hemidactyli* (Lainson and Paperna, 1999) and *I. pardali* (Abdel-Ghaffar *et al.*, 2015) varied in shape from spherical to ovoid. Sporulated oocysts of present *Isospora* species measured 22.48–27.71 × 21.69–26.91 and hence showing close measurement to other *Isospora* spp. such as *I. cannoni*, *I. deserti* (Finkelman and Paperna, 1994), *I. pardali* (Abdel-Ghaffar *et al.*, 2015) and *I. vittati* (Mansour and Abou Shafeey, 2019). However, the current species is bigger than *I. chalchidis*, *I. eimanae* (Amoudi, 1989) and *I. ameivae* (Lainson and Paperna, 1999).

The oocyst wall of species under investigation is bi-layered measuring 1.42–1.78. Bi-layered oocyst wall was also reported in many *Isospora* species such as *I. farahi* (Mihalca *et al.*, 2009), *I. pardali* (Abdel-Ghaffar *et al.*, 2015) and *I. vittati* (Mansour and Abou Shafeey, 2019). However, unilayered oocyst wall was recorded for other species such as *I. ameivae*, and *I. hemidactyli* (Lainson and Paperna, 1999). Oocysts of the present study lack the presence of micropyle, oocyst residuum and polar granule. Similar observations were noticed in oocysts of *I. cannoni*, *I. choochotei* and *I. deserti* (Finkelman and Paperna, 1994), *I. farahi* (Mihalca *et al.*, 2009), *I. pardali* (Abdel-Ghaffar *et al.*, 2015) and *I. vittati* (Mansour and Abou Shafeey, 2019). On the other hand, micropyle was noticed in oocysts *I. eimanae* (Amoudi, 1989) and one polar granule was reported in oocyst of *I. ameivae* and *I. hemidactyli* (Lainson and Paperna, 1999). In addition, few polar granules were reported in oocysts of *I. chalchidis* (Amoudi, 1989).

The sporocysts of the present *Isospora* sp. have ellipsoidal shape, a thin unilayered wall, Stieda body, and a compact residuum. However, sub-Stieda is absent in the present species. These results are in agreement with *I. chalchidis*, *I. eimanae* (Amoudi, 1989), *I. choochotei* (Finkelman and Paperna, 1994) and *I. ameivae* (Lainson and Paperna, 1999). However, Stieda and sub-Stieda bodies are noticed in sporocysts of *I. cannoni*, *I. deserti* (Finkelman and Paperna, 1994), *I. hemidactyli* (Lainson and Paperna, 1999), *I. farahi* (Mihalca *et al.*, 2009) and *I. pardali* (Abdel-Ghaffar *et al.*, 2015). Sporozoite of present isosporan species has a nucleus and two refractile bodies and this appears to be common in sporozoite architecture for many *Isospora* spp. such as *I. cannoni*, *I. choochotei* and *I. deserti* (Finkelman and Paperna, 1994).

The endogenous stages of current *Isospora* sp. occur in the cytoplasm of enterocytes and *lamina propria* of the small intestine of the infected lizards taking an apical position to enterocytes nucleus. Similar results were reported in *I. ameivae* (Lainson and Paperna, 1999), *I. pardali* (Abdel-Ghaffar *et al.*, 2015) and *I. vittati* (Mansour and Abou Shafeey, 2019). However, intranuclear development was recorded for *I. cannoni*, *I. choochotei*, *I. deserti* (Finkelman and Paperna, 1994) and *I. hemidactyli* (Lainson and Paperna, 1999). The present meronts contained up to 34 nuclei and were seen containing up to 10 merozoites. Different shapes and measurements of meronts with different number nuclei and merozoites were observed for many *Isospora* species (Finkelman and Paperna, 1994; Lainson and Paperna, 1999; Abdel-Ghaffar *et al.*, 2015; Mansour and Abou Shafeey, 2019).

After liberation from meronts, merozoites of current *Isospora* sp. invade new cells of the small intestine and develop independently (with no syzygy) into young gamonts. Similar observations are noticed in different members of Eimeriidae (Tenter *et*

al., 2002; Abdel-Ghaffar *et al.*, 2015; Mansour and Abou Shafeey, 2019). The microgamonts of the present investigation contain up to 48 small randomly distributed nuclei while macrogametes are characterized by having a central nucleus and numerous peripherally distributed wall-forming bodies and these results are in agreements with those recorded for many other *Isospora* spp. of reptilian hosts (Lainson and Paperna, 1999; Finkelman and Paperna, 2002; Mihalca *et al.*, 2009; Abdel-Ghaffar *et al.*, 2015).

Finally, further studies are needed to elucidate the ultrastructure of developmental stages of the present haemogregarine and *Isospora* species and molecular characterization of the present three parasites.

Compliance with ethical standards:

All procedures contributing to this work comply with the ethical standards of the relevant national guides on the care and use of laboratory animals and have been approved/authorized by the Institutional Animal Care and Use Committee (IACUC) of Faculty of Science, Cairo University, Egypt.

REFERENCES

Abdel-Ghaffar, F.; Abdel Aziz, A.; El-Toukhy, A. and Abdel-Gawad, M. (1994): Light and electron microscopic studies on blood stages and merogony of *Haemogregarina* sp. infecting the gecko, *Ptyodactylus hasselquistii*. *Journal of the Egyptian German Society of Zoology*, 14(D): 341-363.

Abdel-Ghaffar, F.A.; Shazly, M.A.; El-Habit, O.H.; Gamil, I.S. and Mansour R.M. (2015): Life cycle of *Isospora pardali* sp. nov. (Apicomplexa: Eimeriidae) infecting the leopard fringe-fingered lizard, *Acanthodactylus pardalis* Lichtenstein, 1823 (Reptilia: Lacertidae) in Egypt. *Egyptian Journal of Zoology*, 63(63): 47-68.

Abdel-Haleem, H.M.; Al-Quraishy, S. and Abdel-Baki, A.S. (2013): A redescription of *Haemogregarina damiettae* Ramadan *et al.* 1996 naturally infecting the *Acanthodactylus boskianus* from Egypt, with new merogonic data. *Parasitology Research*, 112: 2045-2048.

Abou-Shafeey, H.E.; Mohamadain, H.S.; Abel-Gaber, R. and Emara, N.M. (2019): Haemogregarines infecting reptiles in Egypt: 1- Blood and merogonic stages of haemogregarine sp. infecting the skink *Scincus scincus*. *Egyptian Journal of Experimental Biology (Zoology)*, 15(2): 127-133.

Alberts, A.C.; Oliva, M.L.; Worley, M.B.; Telford, S.R.; Morris, P.J. and Janssen, D.L. (1998): The need for pre-release health screening in animal translocations: a case study of the Cuban iguana (*Cyclura nubila*). *Animal Conservation*, 1: 165-172.

Al-Hoot, A. and Abd-Al-Aal, Z. (1999): Infection of the Nile monitor *Varanus niloticus niloticus* and the field's horned-viper *Pseudocerastes persicus fieldi* with two *Haemogregarina* spp. (Apicomplexa: haemogregarinidae) in Toshka, Upper Egypt. *Journal of the Egyptian German Society of Zoology*, 29(D): 25-37.

Amoudi, M.A. (1989): Two new species of *Isospora* from the desert skink (*Chalchides ocellatus*) from the Egyptian desert. *Journal of Eukaryotic Microbiology*, 36(3): 237-238.

Baha El Din, S. (2006): A guide to the reptiles and amphibians of Egypt. *The American University in Cairo Press*, pp. 320.

Barta, J.R.; Schrenzel, M.D.; Carreno, R. and Rideout, B.A. (2005): The genus *Atoxoplasma* (Garnham 1950) as a junior objective synonym of the genus *Isospora* (Schneider 1881) species infecting birds and resurrection of *Cystoisospora* (Frenkel 1977) as the correct genus for *Isospora* species

infecting mammals. *Journal of Parasitology*, 91(3): 726-727.

Bashtar, A-R.; Abdel-Ghaffar, F.A. and Shazly, M.A. (1987): Developmental stages of *Hepatozoon gracilis* (Wenyon, 1909) comb. nov., a parasite of the Egyptian skink, *Mabuya quinquetaeniata*. *Parasitology Research*, 73: 507-514.

Bashtar, A-R.; Boulos, R. and Mehlhorn, H. (1984): *Hepatozoon aegypti* nov. sp. 1- life cycle. *Zeitschrift für Parasitenkunde*, 70: 29-41.

Berto, B.P.; Flausino, W.; McIntosh, D.; Teixeira-Filho, W.L. and Lopes, C.W. (2011): Coccidia of New World passerine birds (Aves: Passeriformes): a review of *Eimeria* Schneider, 1875 and *Isospora* Schneider, 1881 (Apicomplexa: Eimeriidae). *Systematic Parasitology*, 80(3): 159-204.

Davies, A.J. and Johnston, M.R. (2000): The biology of some intraerythrocytic parasites of fishes, amphibia, and reptiles. *Advances in Parasitology*, 45:1-107.

Du Toit, P.J. (1937): A new piroplasm (*Sauroplasma thomasi* n. g., n. sp.) of a lizard (*Zonurus giganteus*, Smith). *Onderstepoort Journal of Veterinary Science and Animal Industry*, 9(2): 289-299.

Finkelman, S. and Paperna, I. (1994): The endogenous development of three new intranuclear species of *Isospora* (Apicomplexa: Eimeriidae) from agamid lizards. *Systematic Parasitology*, 27: 213-226.

Finkelman, S. and Paperna, I. (2002): The endogenous development of four new species of *Isospora* Schneider, 1881 (Apicomplexa: Eimeriidae) from Australian geckos. *Systematic Parasitology*, 51: 59-71.

Fuerst, J.A. and Sagulenko, E. (2010): Protein uptake by bacteria: An endocytosis-like process in the planctomycete *Gemmata obscuriglobus*. *Communicative and Integrative Biology*, 3(6): 572-575.

Ghimire, T.R. (2010): Redescription of genera of family Eimeriidae Minchin, 1903. *International Journal of Life Sciences*, 4: 26-47.

Hussien, A.A. (2006): Light and transmission electron microscopic studies of a haemogregarine in naturally infected fan-footed gecko, *Ptyodactylus hasselquistii*. *Parasitology Research*, 98: 468-471.

Karadjian, G.; Chavatte, J. and Landau, I. (2015): Systematic revision of the adeleid haemogregarines, with creation of *Bartazoon* n. g., reassignment of *Hepatozoon argantis* Garnham, 1954 to *Hemolivia*, and molecular data on *Hemolivia stellate*. *Parasite*, 22: 31.

Lainson, R. and Paperna, I. (1999): Redescriptions of *Isospora ameivae* Carini, 1932 in the teiid lizard *Ameiva ameiva* and *Isospora hemidactyli* Carini, 1936 in the gecko *Hemidactylus mabouia*, with particular reference to their endogenous stages. *Memórias do Instituto Oswaldo Cruz*, 94(4): 459-466.

Long, P.L.; Millard, B.J.; Joyner, L.P. and Norton, C.C. (1976): A guide to laboratory techniques used in the study and diagnosis of avian coccidiosis. *Folia Veterinaria Latina*, 6(3): 201-207.

Maia, J.P.; Carranza, S. and Harris, D.J. (2016): Comments on the systematic revision of adeleid haemogregarines: are more data needed?. *Journal of Parasitology*, 102(5): 549-552.

Mansour, R.M. (2020): Light microscopic study of *Caryospora* sp. (Apicomplexa: Eimeriidae) from Savigny's Agama *Trapelus savignii* (Reptilia: Agamidae) in Egypt. *Egyptian Academic Journal of Biological Sciences (E)*, 12(1): 61-76.

Mansour, R.M. and Abou Shafeey, H.E. (2019): Developmental stages of

Isospora vittati n. sp. (Apicomplexa: Eimeriidae) from the bridled skink *Trachylepis vittata* (Reptilia: Scincidae) in Egypt with a checklist of *Isospora* spp. infecting the Egyptian reptiles. *Egyptian Journal of Experimental Biology (Zoology)*, 15(2): 171-182.

Mihalca, A.D.; Jirků, M.; Malonza, P.K. and Modrý, D. (2009): A new species of *Isospora* Schneider, 1881 (Apicomplexa: Eimeriidae) in Ruppell's agama *Agama rueppelli* (Vaillant) (Sauria: Agamidae) from East Africa, with a review of this genus in agamid lizards. *Systematic Parasitology*, 74: 219-223.

Mills, D.B. (2020): The origin of phagocytosis in Earth history. *Interface Focus*, 10(4): 20200019.

Netherlands, E.C.; Cook, C.A.; Du Preez, L.H.; Vanhove, M.P.M.; Brendonck, L. and Smit, N.J. (2020): An overview of the Dactylosomatidae (Apicomplexa: Adeleorina: Dactylosomatidae), with the description of *Dactylosoma kermiti* n. sp. parasitising *Ptychadena anchietae* and *Sclerophrys gutturalis* from South Africa. *International Journal for Parasitology (Parasites and Wildlife)*, 11: 246-260.

Paperna, I.; Kremer-Mecabell, T. and Finkelman, S. (2002): *Hepatozoon kisrae* n. sp. infecting the lizard *Agama stellio* is transmitted by the tick *Hyalomma cf. aegyptium*. *Parasite*, 9(1):17-27.

Reynolds, E.S. (1963): The use of lead citrate at high pH as an electron-opaque stain in electron microscopy. Journal of Cell Biology, 17(1): 208-212.

Shazly, M.A. (2000): Light and electron microscopic studies on the life cycle of *Hepatozoon stellio* sp. nov. 1-erythrocytic stages and merogony inside the Egyptian agamid lizard *Agama stellio*. *Journal of the Egyptian German Society of Zoology*, 31(D): 59-75.

Shazly, M.A. (2003): Erythrocytic and merogonic stages of *Hepatozoon ridibundae* sp. nov. infecting the Arabian ranid frogs, *Rana ridibunda* in Saudi Arabia with reflections on the haemogregarine complex. *Journal of the Egyptian Society of Parasitology*, 33(2): 497-516.

Smith, T.G. (1996): The genus *Hepatozoon* (Apicomplexa: Adeleina). *Journal of Parasitology*, 82(4): 565-585.

Svahn, K. (1976): A new piroplasm *Sauroplasma boreale* sp. n. (Haemosporidia, Theileriidae) from the sand lizard *Lacerta agilis* L. *Norwegian Journal of Zoology*, 24: 1-6.

Telford, S.R., Jr. (2009): Haemogregarines. In: Hemoparasites of the Reptilia: color atlas and text (Telford, S. R., Jr. Ed.). *Taylor and Francis Group, LLC.*, pp. 199-260.

Tenter, A.M.; Barta, J.R.; Beveridge, I.; Duszynski, D.W.; Mehlhorn, H.; Morrison, D.A.; Thompson, R.C. and Conrad, P.A. (2002): The conceptual basis for a new classification of the Coccidia. *International Journal for Parasitology*, 32(5): 595-616.

Ursula, H.; Rüdiger, K.; Frank, M. and Monika, R. (2014): Blood parasites in reptiles imported to Germany. *Parasitology Research*, 113: 4587-4599.

Van As, J. (2012): Ecology, taxonomy and possible life cycles of blood protozoans infecting crag lizards (*Pseudocordylus* spp.) from the eastern Free State highlands. Ph.D. thesis. *The University of the Free State, South Africa*, pp. 232.

Van As, J.; Davies, A.J. and Smit, N.J. (2013): *Hepatozoon langii* n. sp. and *Hepatozoon vacuolatus* n. sp. (Apicomplexa: Adeleorina: Hepatozoidae) from the crag lizard (Sauria: Cordylidae) *Pseudocordylus langi* from the North Eastern

Drakensberg escarpment, Eastern Free State, South Africa. *Zootaxa*, 3608(5): 345-356.

Van As, J.; Davies, A.J. and Smit, N.J. (2015): Life cycle of *Hepatozoon affluomaloti* sp. n. (Apicomplexa: Haemogregarinidae) in crag lizards (Sauria: Cordylidae) and in culicine mosquitoes from South Africa. *Folia Parasitologica (Praha)*, 62: 008 (doi: 10.14411/fp.2015.008).

Votýpka, J.; Modrý, D.; Oborník, M.; Šlapeta, J. and Lukeš, J. (2017): Apicomplexa. In: Handbook of the protists (Archibald, J.M.; Simpson, A.G.B. and Slamovits, C.H. 2nd eds). *Springer International Publishing AG*, pp. 567-624.

ARABIC SUMMARY

نوعين من طفيليات الكوكسيديا ومحتوي سيتوبلازمي فجوي غير إعتيادي داخل كرات الدم الحمراء من سحلية قاضى الجبل الرملى " *Trapelus savignii* " فى مصر

رضا محمد منصور
قسم علم الحيوان والحشرات كلية العلوم جامعة حلوان

تناول هذا البحث تسجيل ثلاثة أنواع من الطفيليات؛ نوعين داخل كرات الدم الحمراء ونوع إيزوسبورا فى سحلية قاضى الجبل الرملى "*Trapelus savignii*" والتى تم تجميعها فى صيف 2019 من الصحراء الشرقية بمصر. وقد إشتملت طفيليات كرات الدم الحمراء فى الدراسة الحالية على نوع هيموجريجارين ومحتويات فجوية ستوبلازمية غير إعتيادية. وقد تميزت مراحل الدم لنوع الهيموجرجارين إلى ثلاثة أشكال وهم التروفوزويت والشكل المتوسط والجامونت الناضج. وقد بلغت قياسات التروفوزويتات 7.50–8.50 (0.30±8.10) × 2.20–2.40 (0.06±2.35) ميكرون بينما سجلت الأطوار المتوسطة والجامونتات البالغة 7.89–10.39 (0.85±9.32) × 3.9–5.18 (0.45±4.32) و8.87–12.13 (0.84±10.25) × 2.50–4.35 (0.58±3.45) ميكرون، بالترتيب. وقد لوحظ عدم إكتساب المحتويات الفجوية السيتوبلازمية داخل كرات الدم الحمراء لصبغة جيمسا أو إكتسابها لون باهت كما سجلت 1.62–5.45 (0.87±3.64) × 1.45–5.35 (1.10±3.51) ميكرون. وعلى مستوى التركيب الدقيق، فقد بدت هذه المحتويات كمادة خلالية شفافة الإلكترون محاطة بغشاء وتحتوي على ثلاثة أنواع من المواد مختلفة الكثافة الإلكترونية والتى ربما تشبه حبيبات الكروماتين. كما لوحظ أيضا عدم وجود نواة أو جهاز جولجى أو ميتوكندريا أو أى تركيب قمي معقد فى هذه المحتويات. وقد تم تسجيل تأثيرات نوع الهيموجريجارين والمحتويات الفجوية السيتوبلازمية على كرات الدم الحمراء المصابة. كما تم أيضاً وصف مراحل التطور الداخلية والخارجية لنوع الإيزوسبورا الحالى. وقد جاءت معظم الأكياس البيضية المتجرثمة كروية الشكل وثنائية الجدار حيث سجلت 22.48–27.71 (1.81±25.47) × 21.69–26.91 (1.73±24.37) ميكرون. وقد لوحظ غياب بقايا الكيس البيضى والحبيبة القطبية والفويهة. وقد جاءت الأكياس الجرثومية بيضاوية الشكل وسجلت 13.79–15.84 (0.67±14.97) × 8.80–11.03 (0.70±9.97). وقد ظهر جسم ستيدا حلمى الشكل وغياب جسم تحت ستيدا. وتحتوى الميرونتات عديدة الأنوية على ما قد يصل إلى 34 نواة وسجلت 6.29 –19.83 (4.58±11.91) × 5.43–10.76 (1.75±7.57) ميكرون. وسجلت الجامونتات المذكرة النامية 16.59–18.89 (0.94±17.74) × 15.61–18.63 (1.24±17.12) ميكرون بينما سجلت الجامونتات المؤنثة البالغة 16.34–24.27 (2.98±19.95) × 12.0–20.28 (3.22±16.92) ميكرون.

````
````